THE JOURNAL OF PHYSICAL CHEMISTRY A
A JOURNAL OF THE AMERICAN CHEMICAL SOCIETY

pubs.acs.org/JPCA Article

CO_2 Activation and Hydrogenation by Palladium Hydride Cluster Anions

Gaoxiang Liu,*,† Zhaoguo Zhu,† Mary Marshall, Moritz Blankenhorn, and Kit H. Bowen*

Cite This: J. Phys. Chem. A 2021, 125, 1747−1753 Read Online

ACCESS | Metrics & More | Article Recommendations | Supporting Information

ABSTRACT: Mass spectrometric analysis of the anionic products of interaction between palladium hydride anions, PdH^-, and carbon dioxide, CO_2, in a reaction cell shows an efficient generation of the $PdHCO_2^-$ intermediate and isolated formate product. Multiple isomers of the $PdHCO_2^-$ intermediates are identified by a synergy between negative ion photoelectron spectroscopy and quantum-chemical calculations. It is shown that a direct mechanism, in which the H atom in PdH^- directly activates and hydrogenates CO_2, leads to the formation of the formate product. An indirect mechanism, on the other hand, leads to a stable $HPdCO_2^-$ structure, where CO_2 is chemisorbed onto the Pd atom.

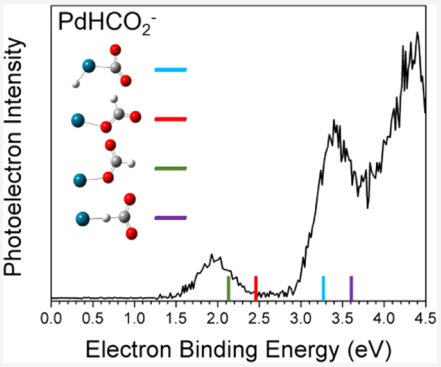

INTRODUCTION

The catalytic conversion of CO_2 into value-added molecules using metal catalysts holds the promise for combating the greenhouse effect caused by the excess amount of CO_2 in the atmosphere. The formation of metal hydrides and the insertion of CO_2 into the metal−hydrogen bond are among the critical steps for CO_2 functionalization over metal catalysts. Comprehensive knowledge about these key steps, however, remains limited as a result of lacking direct experimental characterization on the reaction intermediates.[1−5] Especially, it is less clear how the initial CO_2 interaction with the formed metal hydride can affect the CO_2 activation and the following CO_2 hydrogenation. Mechanistic insight into the CO_2 hydrogenation processes on the active sites is thus deemed essential for the rational design of high-efficiency catalysts for this task.

Via the synergy between the experimental characterization of reaction intermediates and quantum chemistry calculations, gas-phase studies of CO_2 reduction and hydrogenation have provided molecular-level insights into the CO_2 functionalization mechanisms.[6−16] Single- and dual-metal hydrides have been studied for converting CO_2 into formate and formate complexes, shedding light on understanding the mechanisms of CO_2 hydrogenation over various catalysts. As a well-known hydrogen absorber, palladium has been widely applied in catalytic CO_2 functionalization.[17−20] Nevertheless, information on the reaction between palladium hydrides and CO_2 has been scarce. The present work focuses on the hydrogenation of CO_2 via reaction with the anionic palladium monohydride anion, PdH^-. We show that depending on the atom that CO_2 initially interacts with, the reaction ends either in $HPd(CO_2^-)$, in which the CO_2 is activated and bonded to Pd, or in isolated Pd atom and formate, where the formate is released as a final product.

METHODS

Experimental Methods. The present work utilized anion photoelectron spectroscopy (aPES) as its primary probe. The experimental technique, aPES, is conducted by crossing a mass-selected beam of negative ions with a fixed-energy photon beam and energy analyzing the resulting photodetached electrons. This technique is governed by the energy-conservation relationship, $h\nu$ = EBE + EKE, where $h\nu$, EBE, and EKE are the photon energy, electron binding (photodetachment transition) energy, and the electron kinetic energy, respectively. Our photoelectron spectrometer, which has been described previously,[21] consists of one of several ion sources, a linear time-of-flight (TOF) mass spectrometer, a mass gate, a momentum decelerator, a neodymium-doped yttrium aluminum garnet (Nd:YAG) laser for photodetachment, and a magnetic bottle electron energy analyzer. The resolution of the energy analyzer is ∼35 meV at EKE = 1 eV. Photoelectron spectra were calibrated against the well-known photoelectron spectrum of Cu^-.[22]

Received: January 9, 2021
Revised: February 12, 2021
Published: February 23, 2021

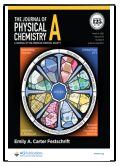

https://dx.doi.org/10.1021/acs.jpca.1c00204
J. Phys. Chem. A 2021, 125, 1747−1753

The PdH^- anion was generated using a pulsed-arc (discharge) cluster ionization source (PACIS), which has been described in detail elsewhere.[23] During PACIS operation, a 30 μs long, 4000 volt electrical pulse applied across the anode and the Pd sample cathode in the discharge chamber vaporizes the palladium atoms.[24] (The sample cathode had been prepared in a nitrogen glove box, where fresh Pd powder was firmly pressed onto a copper rod.) Almost simultaneously with the discharge, 220 psi of ultrahigh purity hydrogen gas was injected into the discharge region, where it was dissociated into hydrogen atoms. The resulting mixture of atoms, ions, and electrons then reacted and cooled as it expanded through the PACIS housing. After a small gap, this flow continued through a 15 cm long collision/reactor cell before exiting into high vacuum. To initiate the reaction between CO_2 and a mixture of PdH^- cluster anions, pure CO_2 was injected into the collision cell using a second pulsed valve. The resultant anions then drifted through a skimmer, through a differentially pumped region, and into the TOF region, where they were perpendicularly extracted and mass-selected prior to photodetachment. Due to palladium's isotope pattern and the presence of multiple hydrogen atoms, photoelectron spectra were taken at all observed mass peaks.

Theoretical Methods. Computations relating to the reactions between carbon dioxide, palladium hydride anions, and the resultant products were performed using the Gaussian 09 program package.[25] Geometry optimizations and frequency calculations were carried out using the hybrid density functional theory (DFT) B3LYP with D3BJ empirical dispersion correction.[26−29] Bond length of PdH^- anion optimized at B3LYP level was found to be 1.538 Å, which perfectly matches the previous result 1.538 Å at PBEPBE level.[13] The vertical detachment energy (VDE) of the optimized structures were calculated using B3LYP DFT functional with the unrestricted Kohn−Sham solution, and then improved by single point energy calculations at the coupled-cluster single, double, and perturbative triple CCSD(T) level of theory.[30] Natural population analysis (NPA) was conducted to examine the charge distribution at the B3LYP level using natural bond orbital (NBO) 3.1 implemented in Gaussian 09.[31] NPA has been found to be satisfactory in predicting charge distributions within metal clusters.[32,33] The initially estimated structures for transition states (TS) were obtained by selecting appropriate coordinates from relaxed potential energy surface scans. Vibrational frequencies were calculated to determine whether the stationary points were local minima or transition states. The intrinsic reaction coordinate (IRC) calculations were carried out to make sure that a TS connects two appropriate minima.[34,35] The aug-cc-pwCVTZ-DK (for Pd) and aug-cc-PVTZ-DK basis sets (for C, H, O) and the second-order Douglas−Kroll−Hess (DKH2) scalar relativistic Hamiltonian were used throughout our computations.[36−41]

RESULTS AND DISCUSSION

The TOF mass spectra without and with CO_2 pulsed into the reaction cell are shown in the top and bottom panel of Figure 1, respectively. Without CO_2 in the cell, PdH^- and $PdCO^-$ are observed in the mass spectrum. The presence of $PdCO^-$ is due to carbon and oxygen absorbed onto the palladium powder. Note that PdH^- is the only palladium hydride anion that is observed under this experimental condition. At higher mass, a mass series of $PdH_xCO_2^-$ appears after CO_2 is introduced into

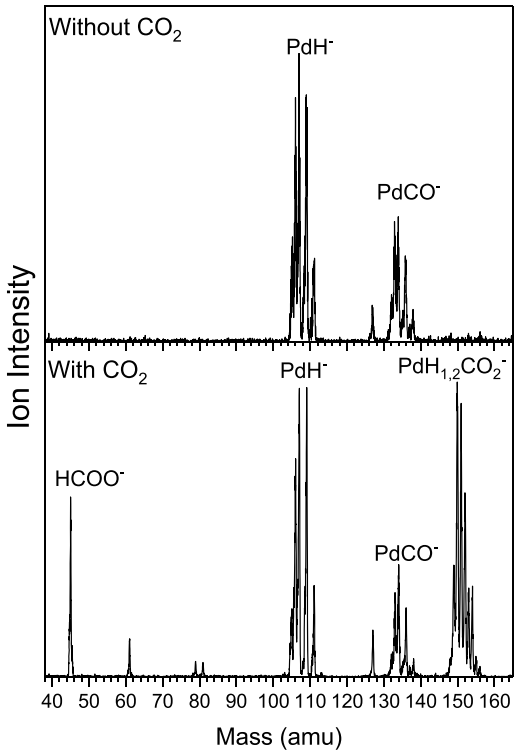

Figure 1. Mass spectra of anions generated by PACIS without (top panel) and with (bottom panel) CO_2 injection into the cell.

the reaction cell. We expanded this region and compared it with the simulated mass spectra of $PdH_1CO_2^-$ and $PdH_2CO_2^-$ (Figure 2). This comparison suggests that $PdH_xCO_2^-$ is a mixture of both $PdH_1CO_2^-$ and $PdH_2CO_2^-$. At lower mass in Figure 1, a peak at 45 amu can be observed after adding CO_2 into the reaction cell. Photoelectron spectroscopy confirmed this anion as the formate, $HCOO^-$ (Figure S1). The formation of the formate anion suggests that CO_2 is hydrogenated upon interaction with PdH^-, and that the formate product is released after the hydrogenation is complete. $PdH_1CO_2^-$, on the other hand, represents a key reaction intermediate when PdH^- hydrogenates CO_2. Better characterization of this intermediate would help to understand the hydrogenation mechanism.

To characterize this reaction intermediate, we identified the mass peaks that solely consist of $PdH_1CO_2^-$ (Figure 2), mass-selected these peaks, and performed negative ion photoelectron spectroscopy on them. The photoelectron spectrum of $PdHCO_2^-$ taken with a 266 nm (4.66 eV) laser is presented in Figure 3. It shows three bands spanning from 1.5 to 4.5 eV. Their peak positions, 2.02, 3.34, and 4.41 eV, are, respectively, assigned as their vertical detachment energies (VDE). The VDE is defined as the photodetachment transition energy at which the Franck−Condon overlap is at its maximum between the anion's vibrational wave function and that of its neutral counterpart with both in their ground electronic states.

Figure 4 presents four calculated structures of $PdHCO_2^-$ that may be made by the reaction between PdH^- and CO_2. All structures are in their singlet states, while the triplet states are significantly higher in energy. Isomer A is the most stable structure. The H atom and the C atom of CO_2 bond with the Pd atom. CO_2 is significantly bent, being activated on the Pd atom. Isomers B, C, and D all have a formate moiety attached to Pd. They are, respectively, 0.83, 0.84, and 1.20 eV higher in

https://dx.doi.org/10.1021/acs.jpca.1c00204
J. Phys. Chem. A 2021, 125, 1747−1753

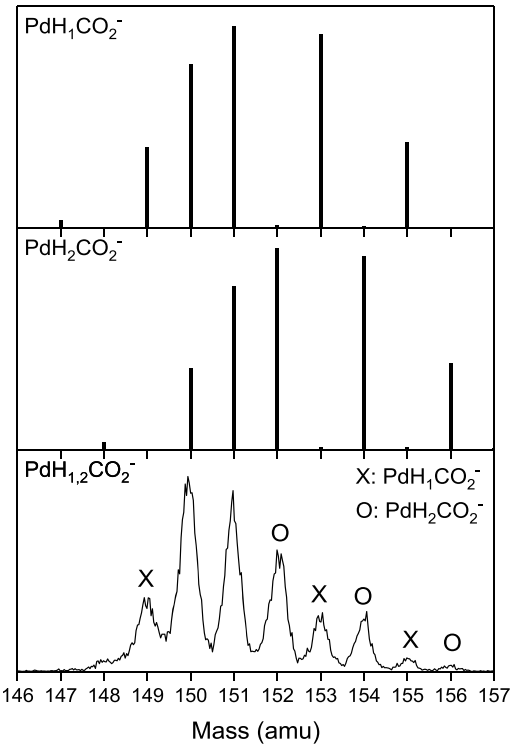

Figure 2. Simulated and experimental mass spectra of $PdHCO_2^-$ and $PdH_2CO_2^-$. The peaks marked by a cross indicate peaks consisting of only $PdHCO_2^-$, while peaks marked with a circle indicate peaks consisting of only $PdH_2CO_2^-$.

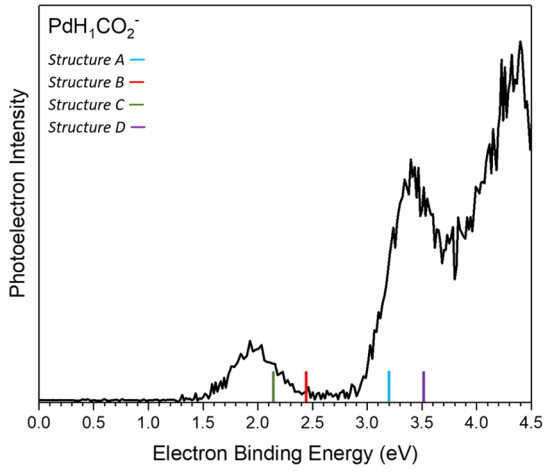

Figure 3. Photoelectron spectrum of $PdHCO_2^-$ measured with 266 nm (4.66 eV) photons. The stick spectrum overlay represents the calculated VDE values of the different $PdHCO_2^-$ structures in Figure 4.

energy than isomer A. Isomers B and C are two conformers by rotating the longer C−O bond, where the oxygen atom connects palladium. The C−H bond lengths in isomers B and C are both 1.12 Å, close to that of an isolated HCO_2^- anion (1.17 Å). Unlike other isomers which have planar geometries, structure D has a small Pd−H−CO_2 dihedral angle of 7.33°. The H atom in structure (isomer) D bridges the Pd and the C atoms.

To verify the calculated structures, we compare their calculated VDE to the experimental ones. The feature in the low EBE region (1.5−2.5 eV) of Figure 3 can be attributed to

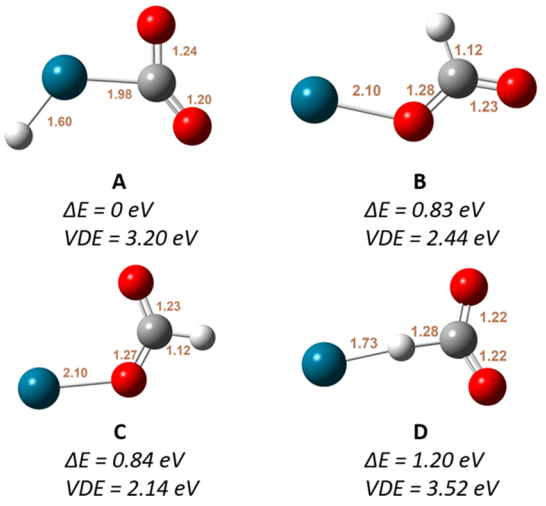

Figure 4. Optimized structures of $PdHCO_2^-$. The relative energies of $PdHCO_2^-$ and their calculated VDEs are listed below each structure. Bond lengths are also shown in each structure.

the photodetachment of isomers B and C. The calculated VDE values of isomers A and D are 3.20 and 3.52 eV, respectively, matching the second band (3.0−3.7 eV). This band, which peaked at EBE = 3.34 eV, can also originate from a transition between the anion and the neutral excited states of structure B (Table S1).

The mechanism of CO_2 hydrogenation by PdH^- was investigated by quantum-chemical calculations. Figure 5 presents the possible reaction pathways for CO_2 activation and hydrogenation by PdH^-. For Path A, the reaction starts with the charge transfer from PdH^- to CO_2 via the interaction between Pd and C and proceeds to **IT1** (structure A). The partial charge on the CO_2 moiety in **IT1** is −0.52 e, indicating that CO_2 is significantly reduced. This CO_2 activation process is barrierless and exothermic by 1.34 eV. In order for **IT1** to convert CO_2 into formate, the H atom needs go beyond the Pd−CO_2 plane to transfer onto the CO_2 moiety. This is achieved by rotation of the single Pd−C bond that breaks planar geometry and by stretching between the H and C atoms to form the Pd−H−C triangle (**TS1**). After overcoming **TS1**, the H atom connects the Pd atom and the CO_2 moiety, forming **IT2** (structure D). The barrier for this step is 1.10 eV. Energetically, **TS1** is lower than **IT2** by 0.1 eV at the CCSD(T) level but 0.04 eV higher at the DFT level. This often indicates a negligible barrier (relative to **IT2**).[12] Rather than via **IT1** and **TS1**, the reaction can also proceed through the direct interaction between the H atom and CO_2 to form **IT2**, i.e., through Path B. This step is exothermic by 0.14 eV. This path represents a direct CO_2 attachment mechanism, which has been found in CO_2 hydrogenation by FeH^- and $Cu_2H_2^-$.[12,13] After formation, **IT2** can convert to **IT3** (structure B) over a very small barrier (0.01 eV). Therefore, **IT2** can easily reorient itself to **IT1** or **IT3**. As Pd approaches O, breakage of the Pd−H bond contributes to the formation of the formate moiety in intermediate **IT3**. After getting over the rotation barrier of 0.14 eV, **IT3** becomes its conformal isomer **IT4** (structure C). The dissociation process of intermediate **IT3/4** into the palladium atom and formate anion is endothermic by 1.05/1.04 eV. Thus, all intermediates and transition states are below the entrance channel, and the complete hydrogenation reaction is endothermic by 0.54 eV

https://dx.doi.org/10.1021/acs.jpca.1c00204
J. Phys. Chem. A 2021, 125, 1747−1753

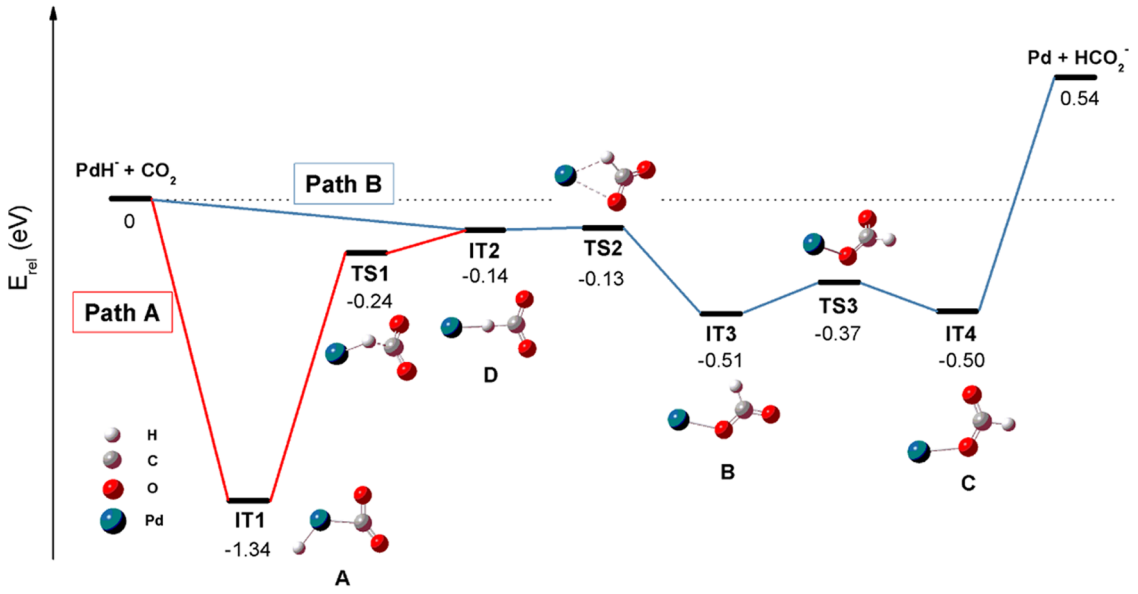

Figure 5. Calculated reaction pathway for CO_2 hydrogenation by PdH^-. Zero-point corrected energies are given in eV. The total energy of isolated PdH^- and CO_2 is set at 0 eV.

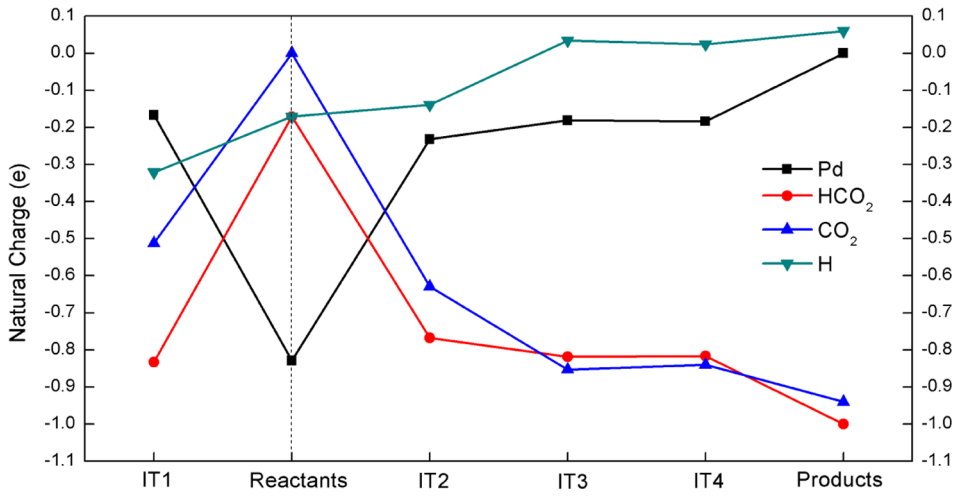

Figure 6. Charges on different moieties of $PdHCO_2^-$ intermediates along the reaction pathway of CO_2 activation by PdH^-.

above it. This energetics makes the whole reaction accessible under the multicollision environment in the reaction cell, where excess energy is provided by colliding with the fastest-moving H_2 molecules within the Boltzman distribution.[15,42−44]

Figure 6 maps the evolution of natural charges on different atoms/moieties of $PdHCO_2^-$ Essentially, it shows that the electron required to reduce the CO_2 molecule comes from the Pd atom. From reactants to **IT1**, the charge on the CO_2 moiety (in blue) plummets by 0.512 e, indicating that CO_2 is activated in the first step of Path A. To the right of reactants in Figure 6, i.e., along Path B, significant electron transfer (0.629 e) from PdH^- to the CO_2 moiety (in blue) is induced by the direct attachment of CO_2 onto PdH^-. The black line (for Pd) soars from −0.829 to −0.232 e between reactants and **IT2**, which means that the negative charge needed to reduce CO_2 mainly originates from the palladium atom as well. The downhill side of the blue line (CO_2) from reactants to **IT3** shows that the negative charge accumulates on the CO_2 moiety as the reaction proceeds. After surmounting **TS2**, the natural charge on the CO_2 moiety in **IT3** and **IT4** is −0.85 and −0.84 e, close to the −0.94 e on CO_2 in free formate anion, revealing that CO_2 is fully activated and the hydrogenation process is complete.

Additionally, hydride affinities of metal atoms provide a different perspective for the mechanism of CO_2 insertion into the metal−hydrogen bond. Considering the simplest model, M−H, bond dissociation energies (BDE) of Fe−H, Pt−H, and Pd−H are 1.63, 3.44, and 2.44 eV, respectively.[45−47] The highest hydride affinity (3.44 eV) may account for the high barrier of CO_2 insertion into the Pt−H bond.[11] Moreover, the lower energy barrier of CO_2 insertion into Pd−H (1.10 eV), compared to that of Pt−H (2.84 eV), explains why CO_2 insertion is allowed in the $PdH^- + CO_2$ reaction but forbidden in the $PtH^- + CO_2$ case. In the case of FeH^-, the direct CO_2 attachment to the H atom dominates as a result of the low Fe−H bond dissociation energy (1.63 eV). For the $PdH^- + CO_2$ reaction, on the other hand, its intermediate Pd−H BDE (2.44 eV) renders possible both indirect and direct hydrogenation paths (Paths A and B).

We also investigated the $PdH_2CO_2^-$ anion that appeared in the experiment. Figure 7 shows the photoelectron spectrum of

https://dx.doi.org/10.1021/acs.jpca.1c00204
J. Phys. Chem. A 2021, 125, 1747−1753

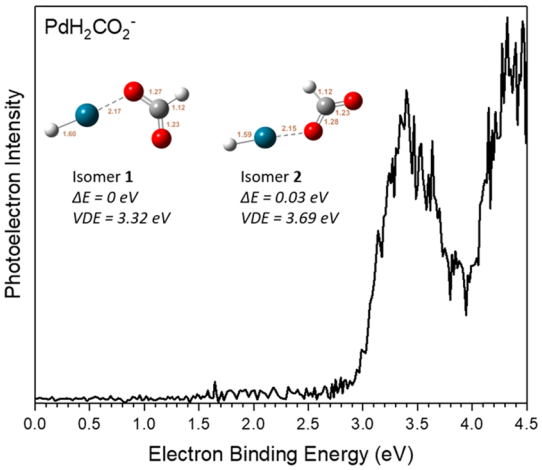

Figure 7. Photoelectron spectrum of $PdH_2CO_2^-$ measured with 266 nm (4.66 eV) photons. Lowest-energy isomeric structures are displayed for each isomer. The relative energies of $PdH_2CO_2^-$ and their calculated VDEs are listed below each structure. Bond lengths are also shown in each structure.

$PdH_2CO_2^-$ anion measured with 466 nm photons, as well as the lowest-energy structures. Two broad transitions, which peaked at EBE of 3.40 and 4.34 eV, were observed in the spectrum. Thus, the VDE value for $PdH_2CO_2^-$ is 3.40 eV. The feature beyond the first peak depicts transitions from ground states of the anions to the electronically excited states of the corresponding neutrals. Optimized isomers **1** and **2** both have PdH and formate moieties, suggesting that $PdH_2CO_2^-$ is likely due to the reaction between PdH neutral molecules and formate anions. NBO analysis shows that the net charge on the Pd−H moiety is only −0.16 e in both isomer **1** and **2** structures, this indicating that $PdH_2CO_2^-$ is a [PdH-($COOH^-$)] adduct. The computed VDE values of isomers **1** and **2** are 3.32 and 3.69 eV, respectively, in agreement with the experimental result.

CONCLUSIONS

We have demonstrated that the activation of CO_2 followed by its hydrogenation can be accomplished in the gas phase by palladium hydride anions. Both the activation intermediate, $PdHCO_2^-$, and the hydrogenation product, HCO_2^-, were observed in the mass spectrum. The combination of anion photoelectron spectroscopy and quantum-chemical calculation identified multiple isomers of the $PdHCO_2^-$ intermediates. Mechanistic analysis reveals that direct activation of CO_2 through H−C bond formation is barrierless and leads to the hydrogenated product, HCO_2^-, while the attachment of CO_2 onto the palladium atom side of PdH^- leads to a stable H−Pd−CO_2^- structure. Charge analysis shows that the electron needed to activate CO_2 comes from the palladium atom. This work provides molecular-level insight into the nature of CO_2 hydrogenations with metal hydrides, shedding light on the properties of metal-based catalysis in the condensed phase.

ASSOCIATED CONTENT

Supporting Information

The Supporting Information is available free of charge at https://pubs.acs.org/doi/10.1021/acs.jpca.1c00204.

Details of additional experimental and theoretical results, including photoelectron spectrum of formate anion; excitation energies of neutral $PdH_{1,2}CO_2$; and Cartesian coordinates of optimized structures (PDF)

AUTHOR INFORMATION

Corresponding Authors

Gaoxiang Liu − *Department of Chemistry, Johns Hopkins University, Baltimore, Maryland 21218, United States;* orcid.org/0000-0002-1001-0064; Email: gaoxiangliu@berkeley.edu

Kit H. Bowen − *Department of Chemistry, Johns Hopkins University, Baltimore, Maryland 21218, United States;* orcid.org/0000-0002-2858-6352; Email: kbowen@jhu.edu

Authors

Zhaoguo Zhu − *Department of Chemistry, Johns Hopkins University, Baltimore, Maryland 21218, United States;* orcid.org/0000-0002-4395-9102

Mary Marshall − *Department of Chemistry, Johns Hopkins University, Baltimore, Maryland 21218, United States*

Moritz Blankenhorn − *Department of Chemistry, Johns Hopkins University, Baltimore, Maryland 21218, United States*

Complete contact information is available at: https://pubs.acs.org/10.1021/acs.jpca.1c00204

Author Contributions

†G.L. and Z.Z. contributed equally to this manuscript.

Notes

The authors declare no competing financial interest.

ACKNOWLEDGMENTS

This material is based upon the work supported by the Air Force Office of Scientific Research (AFOSR) under Grant No. FA9550-19-1-0077 (K.H.B.).

REFERENCES

(1) Tang, Q.; Lee, Y.; Li, D.-Y.; Choi, W.; Liu, C. W.; Lee, D.; Jiang, D. Lattice-Hydride Mechanism In Electrocatalytic CO_2 Reduction By Structurally Precise Copper-Hydride Nanoclusters. *J. Am. Chem. Soc.* **2017**, *139*, 9728−9736.

(2) Zhu, S.; Jiang, B.; Cai, W.; Shao, M. Direct Observation On Reaction Intermediates And The Role Of Bicarbonate Anions In CO_2 Electrochemical Reduction Reaction On Cu Surfaces. *J. Am. Chem. Soc.* **2017**, *139*, 15664−15667.

(3) Mori, K.; Sano, T.; Kobayashi, H.; Yamashita, H. Surface Engineering Of A Supported Pdag Catalyst For Hydrogenation Of CO_2 To Formic Acid: Elucidating The Active Pd Atoms In Alloy Nanoparticles. *J. Am. Chem. Soc.* **2018**, *140*, 8902−8909.

(4) Kato, S.; Matam, S. K.; Kerger, P.; Bernard, L.; Battaglia, C.; Vogel, D.; Rohwerder, M.; Zuttel, A. The Origin Of The Catalytic Activity Of A Metal Hydride In CO_2 Reduction. *Angew. Chem., Int. Ed.* **2016**, *55*, 6028−6032.

(5) Wang, W.; Himeda, Y.; Muckerman, J. T.; Manbeck, G. F.; Fujita, E. CO_2 Hydrogenation To Formate And Methanol As An Alternative To Photo-And Electrochemical CO_2 Reduction. *Chem. Rev.* **2015**, *115*, 12936−12973.

(6) Green, A. E.; Justen, J.; Schöllkopf, W.; Gentleman, A. S.; Fielicke, A.; Mackenzie, S. R. IR Signature of Size-Selective CO_2 Activation on Small Platinum Cluster Anions, Pt_n−(n= 4−7). *Angew. Chem., Int. Ed.* **2018**, *57*, 14822−14826.

(7) Liu, G.; Ciborowski, S. M.; Zhu, Z.; Chen, Y.; Zhang, X.; Bowen, K. H. The Metallo-Formate Anions, M (CO_2)−, M.= Ni, Pd, Pt, Formed By Electron-Induced CO_2 Activation. *Phys. Chem. Chem. Phys.* **2019**, *21*, 10955−10960.

(8) Liu, G.; Ariyarathna, I.; Ciborowski, S. M.; Zhu, Z.; Miliordos, E.; Bowen, K. H. Simultaneous Functionalization of Methane and Carbon Dioxide Mediated by Single Platinum Atomic Anions. *J. Am. Chem. Soc.* **2020**, *142*, 21556−21561.
(9) Thompson, M. C.; Ramsay, J.; Weber, J. M. Solvent-Driven Reductive Activation of CO_2 By Bismuth: Switching From Metalloformate Complexes To Oxalate Products. *Angew. Chem., Int. Ed.* **2016**, *55*, 15171−15174.
(10) Tang, S.; Rijs, N. J.; Li, J.; Schlangen, M.; Schwarz, H. Ligand Controlled CO_2 Activation Mediated by Cationic Titanium Hydride Complexes,[LTiH]+(L= Cp2, O). *Chem. - Eur. J.* **2015**, *21*, 8483−8490.
(11) Zhang, X.; Liu, G.; Meiwes-Broer, K.; Gantefor, G.; Bowen, K. CO_2 Activation and Hydrogenation by Pth_n^- Cluster Anions. *Angew. Chem., Int. Ed.* **2016**, *55*, 9644−9647.
(12) Jiang, L.; Zhao, C.; Li, X.; Chen, H.; He, S.-G. Formation of Gas-Phase Formate in Thermal Reactions of Carbon Dioxide with Diatomic Iron Hydride Anions. *Angew. Chem., Int. Ed.* **2017**, *56*, 4187−4191.
(13) Liu, Y.-Z.; Jiang, L.-X.; Li, X.-N.; Wang, L.-N.; Chen, J.-J.; He, S.-G. Gas-Phase Reactions Of Carbon Dioxide with Copper Hydride Anions $Cu_2H_2^-$: Temperature-Dependent Transformation. *J. Phys. Chem. C* **2018**, *122*, 19379−19384.
(14) Pascher, T. F.; Oncak, M.; van der Linde, C.; Beyer, M. K. Release of Formic Acid from Copper Formate: Hydride, ProtonCoupled Electron and Hydrogen Atom Transfer All Play their Role. *ChemPhysChem* **2019**, *20*, 1420−1424.
(15) Liu, G.; Poths, P.; Zhang, X.; Zhu, Z.; Marshall, M.; Blankenhorn, M.; Alexandrova, A. N.; Bowen, K. H. CO_2 Hydrogenation to Formate and Formic Acid by Bimetallic Palladium−Copper Hydride Clusters. *J. Am. Chem. Soc.* **2020**, *142*, 7930−7936.
(16) McMahon, A. J.; Jarrold, C. C. Using Anion Photoelectron Spectroscopy of Cluster Models to Gain Insights Into Mechanisms Of Catalyst-Mediated H_2 Production From Water. *Phys. Chem. Chem. Phys.* **2020**, 27936−27948.
(17) Song, H.; Zhang, N.; Zhong, C.; Liu, Z.; Xiao, M.; Gai, H. Hydrogenation of CO_2 into Formic Acid Using a Palladium Catalyst on Chitin. *New J. Chem.* **2017**, *41*, 9170−9177.
(18) Qian, C.; Sun, W.; Hung, D. L.; Qiu, C.; Makaremi, M.; Kumar, S. G. H.; Wan, L.; Ghoussoub, M.; Wood, T. E.; Xia, M.; et al. Catalytic CO_2 Reduction by Palladium-Decorated Silicon−Hydride Nanosheets. *Nat. Catal.* **2019**, *2*, 46−54.
(19) Li, N.; Liu, M.; Yang, B.; Shu, W.; Shen, Q.; Liu, M.; Zhou, J. Enhanced Photocatalytic Performance Toward CO_2 Hydrogenation over Nanosized Tio_2-Loaded Pd under UV Irradiation. *J. Phys. Chem. C* **2017**, *121*, 2923−2932.
(20) Ma, Y.; Ren, Y.; Zhou, Y.; Liu, W.; Baaziz, W.; Ersen, O.; Pham-Huu, C.; Greiner, M.; Chu, W.; et al. High-Density and Thermally Stable Palladium Single-Atom Catalysts for Chemoselective Hydrogenations. *Angew. Chem., Int. Ed.* **2020**, *59*, 21613−21619.
(21) Gerhards, M.; Thomas, O. C.; Nilles, J. M.; Zheng, W.−J.; Bowen, K. H. Cobalt−Benzene Cluster Anions: Mass Spectrometry and Negative Ion Photoelectron Spectroscopy. *J. Chem. Phys.* **2002**, *116*, No. 10247.
(22) Ho, J.; Ervin, K. M.; Lineberger, W. C. Photoelectron Spectroscopy of Metal Cluster Anions: Cu−N, Ag−N, and Au−N. *J. Chem. Phys.* **1990**, *93*, 6987−7002.
(23) Zhang, X.; Liu, G.; Ganteför, G.; Bowen, K. H.; Alexandrova, A. N. $PtZnH_5^-$, a σ-aromatic Cluster. *J. Phys. Chem. Lett.* **2014**, *5*, 1596−1601.
(24) Zhang, X.; Robinson, P. J.; Ganteför, G.; Alexandrova, A. N.; Bowen, K. H. Photoelectron Spectroscopic and Theoretical Study of the [HPd (η2-H_2)]− Cluster Anion. *J. Chem. Phys.* **2015**, *143*, No. 094307.
(25) Frisch, M. J.; Trucks, G. W.; Schlegel, H. B.; Scuseria, G. E.; Robb, M. A.; Cheeseman, J. R.; Scalmani, G.; Barone, V.; Mennucci, B.; Petersson, G. A. et al. *Gaussian 09*, revision D.01; Gaussian, Inc.: Wallingford, CT, 2013.
(26) Lee, C. T.; Yang, W. T.; Parr, R. G. Development of the Collesalvetti Correlation−Energy Formula into a Functional of the Electrondensity. *Phys. Rev. B* **1988**, *37*, 785−789.
(27) Becke, A. D. Density−Functional Exchange−Energy Approximation with Correct Asymptotic−Behavior. *Phys. Rev. A* **1988**, *38*, 3098−3100.
(28) Becke, A. D. Density−Functional Thermochemistry. III. The Role of Exact Exchange. *J. Chem. Phys.* **1993**, *98*, 5648−5652.
(29) Grimme, S.; Antony, J.; Ehrlich, S.; Krieg, H. A Consistent and Accurate Ab Initio Parametrization of Density Functional Dispersion Correction (DFT−D) for the 94 Elements H−Pu. *J. Chem. Phys.* **2010**, *132*, No. 154104.
(30) Raghavachari, K.; Trucks, G. W.; Pople, J. A.; Head−Gordon, M. A Fifth−Order Perturbation Comparison of Electron Correlation Theories. *Chem. Phys. Lett.* **1989**, *157*, 479−483.
(31) Glendening, E. D.; Reed, A. E.; Carpenter, J. E.; Weinhold, F. *NBO*, version 3.1, 1998.
(32) Wang, H.; Zhang, X.; Ko, Y. J.; Grubisic, A.; Li, X.; Ganteför, G.; Schnöckel, H.; Eichhorn, B. W.; Lee, M. S.; Jena, P.; et al. Aluminum Zintl Anion Moieties Within Sodium Aluminum Clusters. *J. Chem. Phys.* **2014**, *140*, No. 054301.
(33) Wang, H.; Jae Ko, Y.; Zhang, X.; Gantefoer, G.; Schnoeckel, H.; Eichhorn, B. W.; Jena, P.; Kiran, B.; Kandalam, A. K.; Bowen, K. H. The Viability of Aluminum Zintl Anion Moieties Within Magnesium-Aluminum Clusters. *J. Chem. Phys.* **2014**, *140*, No. 124309.
(34) Gonzalez, C.; Schlegel, H. B. An Improved Algorithm for Reaction−Path Following. *J. Chem. Phys.* **1989**, *90*, 2154−2161.
(35) Gonzalez, C.; Schlegel, H. B. Reaction−Path Following in Mass−Weighted Internal Coordinates. *J. Phys. Chem. A* **1990**, *94*, 5523−5527.
(36) Peterson, K. A.; Figgen, D.; Dolg, M.; Stoll, H. Energy−Consistent Relativistic Pseudopotentials and Correlation Consistent Basis Sets for the 4d Elements Y−Pd. *J. Chem. Phys.* **2007**, *126*, No. 124101.
(37) Dunning, T. H. Gaussian Basis Sets for Use in Correlated Molecular Calculations. I. The Atoms Boron Through Neon and Hydrogen. *J. Chem. Phys.* **1989**, *90*, 1007−1023.
(38) De Jong, W. A.; Harrison, R. J.; Dixon, D. A. Parallel Douglas−Kroll Energy and Gradients in Nwchem: Estimating Scalar Relativistic Effects Using Douglas−Kroll Contracted Basis Sets. *J. Chem. Phys.* **2001**, *114*, 48−53.
(39) Kendall, R. A.; Dunning, T. H.; Harrison, R. J. Electron Affinities of the First-Row Atoms Revisited. Systematic Basis Sets and Wave Functions. *J. Chem. Phys.* **1992**, *96*, 6796−6806.
(40) Douglas, M.; Kroll, N. M. Quantum Electrodynamical Corrections to the Fine Structure of Helium. *Ann. Phys.* **1974**, *82*, 89−115.
(41) Reiher, M.; Wolf, A. Exact Decoupling of the Dirac Hamiltonian. II. The Generalized Douglas-Kroll-Hess Transformation up to Arbitrary Order. *J. Chem. Phys.* **2004**, *121*, No. 10945.
(42) Liu, G.; Zhu, Z.; Ciborowski, S. M.; Ariyarathna, I. R.; Miliordos, E.; Bowen, K. H. Selective Activation of the C−H Bond in Methane by Single Platinum Atomic Anions. *Angew. Chem., Int. Ed.* **2019**, *58*, 7773−7777.
(43) Liu, G.; Ciborowski, S.; Bowen, K. H. Photoelectron Spectroscopic and Computational Study of Pyridine-Ligated Gold Cluster Anions. *J. Phys. Chem. A* **2017**, *121*, 5817−5822.
(44) Liu, G.; Miliordos, E.; Ciborowski, S. M.; Tschurl, M.; UBoesl, U.; Heiz, U.; Zhang, X.; Xantheas, S. S.; Bowen, K. H. Communication: Water activation and splitting by single metal-atom anions. *J. Chem. Phys.* **2018**, *149*, No. 221101.
(45) Schultz, R. H.; Armentrout, P. B. The Gas-Phase Thermochemistry of FeH. *J. Chem. Phys.* **1991**, *94*, 2262−2268.
(46) Mccarthy, M. C.; Field, R. W.; Engleman, R.; Bernath, P. F. Laser and Fourier transform spectroscopy of PtH and PtD. *J. Mol. Spectrosc.* **1993**, *158*, 208−236.
(47) Tolbert, M. A.; Beauchamp, J. L. Homolytic And Heterolytic Bond Dissociation Energies of the Second Row Group 8, 9, and 10

https://dx.doi.org/10.1021/acs.jpca.1c00204
J. Phys. Chem. A 2021, 125, 1747−1753

Diatomic Transition−Metal Hydrides: Correlation With Electronic Structure. *J. Chem. Phys.* **1986**, *90*, 5015−5022.

https://dx.doi.org/10.1021/acs.jpca.1c00204
J. Phys. Chem. A 2021, 125, 1747−1753